

## **A study on the generation of stress and strain in geotextile tube by scale model test**

Hyeong-Joo Kim<sup>1)</sup>, Myoung-Soo Won<sup>2)</sup>, Jang-Baek Lee<sup>3)</sup>, Min-Jun Choi<sup>4)</sup>  
and \*Jay C. Jamin<sup>5)</sup>

<sup>1), 2)</sup> *Department of Civil Engineering, Kunsan National University, Gunsan 573-701, Korea*

<sup>3), 4), 5)</sup> *Department of Civil and Environmental Engineering, Kunsan National University, Gunsan 573-701, Korea*

<sup>1)</sup> [kimhj@kunsan.ac.kr](mailto:kimhj@kunsan.ac.kr)

<sup>2)</sup> [wondain@kunsan.ac.kr](mailto:wondain@kunsan.ac.kr)

<sup>3)</sup> [leejb@kunsan.ac.kr](mailto:leejb@kunsan.ac.kr)

<sup>4)</sup> [minjun1208@gmail.com](mailto:minjun1208@gmail.com)

<sup>5)</sup> [jaminjc@kunsan.ac.kr](mailto:jaminjc@kunsan.ac.kr)

### **ABSTRACT**

Geotextile tubes are tubular structures made of strong permeable material which are hydraulically or mechanically filled with dredged material. Geotextile tubes are made of permeable woven or non-woven synthetic fibers (i.e. polyester or PET and polypropylene or PP). Geotextile tubes have been widely applied in environmental and coastal engineering as alternatives for the conventional concrete-made structures such as containment dikes, revetments, levees, groins, seawalls and breakwaters. The geotextile tube's performance in strength, dewatering, retaining solid particles and stacked stability have been studied extensively in the past. However, only little research have been done regarding the generation of stress and strain in geotextile tubes. In this paper, a scale model test was conducted on a 4 m long geotextile tube with a theoretical diameter of 1 m. The test was conducted using a large scale apparatus designed to simulate actual field conditions. The apparatus is equipped with a slurry mixing station, pumping and delivery station, an observation station and a data station. Load cells placed at the inner belly of the geotextile tube to monitor the total soil pressure. Strain gauges were also placed on the outer skin of the tube to measure the geotextile strain. The pressure and strain sensors are attached to a data logger which sends the collected data to a desktop computer. Test results showed that the total horizontal pressures are higher than the total vertical pressures. Also, the geotextile stains at the sides of the geotextile tube are larger than the geotextile strains on the top. This implies that the increase in the geotextile strains at the sides of the tube corresponds to the increase in the lateral pressure induced by the fill material.

---

<sup>1)</sup> Professor

<sup>2)</sup> Assistant Professor

<sup>3), 5)</sup> Ph.D. candidate

<sup>4)</sup> Graduate student

## **1. INTRODUCTION**

Geotextile tubes are widely used in South Korea since the late 1990's up to the present. Presently, the annual consumption of cement and concrete has significantly increased in South Korea. There is a decreasing supply of cement and construction aggregates such as rock, gravel and sand whose quantities are now limited due to environmental restrictions in the quarry site. Construction expenses have also increased due to additional delivery costs from source to site and construction time is longer due to may process and equipment involved. Geotextile tube technology could be a viable alternative to the conventional rubble mound structures in cases where temporary protection is required or rock is not obtainable and difficult to transport to the site.

Geotextile tubes are made from strong and flexible textile materials that are capable of retaining fine-grained materials though permeable enough to allow the excess water from the hydraulically filled slurry to dissipate. In recent years geotextile tubes were used as groins and breakwaters to protect or mitigate shoreline/coastline erosions (Cantré, 2002; Gibeaut et al., 2003; Alvarez et al., 2007; Pilarczyk, 2008; Parab et al., 2011), as containment dikes for land reclamation and man-made islands (Fowler et al., 2002a; 2002b), and as revetments acting as mass-gravity barrier-type structures and protection dikes to prevent damage to valuable structures caused by natural calamities (Restall et al., 2002; Lawson, 2008).

Geotextile tubes has been of interest in various studies due to its wide applications in civil engineering. Laboratory evaluation results on the permeability and retention characteristics of geotextiles can be found in the studies of Moo-Young et al. (2002), Koerner & Koerner (2006), Weggel et al. (2011) and Vashi et al. (2013). Model tests and large-scale experiments on geotextile tubes can be found in the literature (Recio & Oumeraci, 2009; Kriel, 2012; Kim et al., 2013b, 2014a, 2014b). Numerical (Kim et al., 2013a, 2014b) & analytical methods (Plaut & Klusman, 1999) were also conducted to study the stability of stacked geotextile tubes. In general the studies available in the literature focuses on the investigation of the hydraulic stability of stacked geotextile tubes and the geotextile performance in strength, durability and permeability. However, very little is presently understood about the consolidation behavior of the fill materials and the stress and strain behavior of the confining geotextile. Brink et al. (2013; 2015) has proposed a consolidation modeling method for geotextile tubes filled with fine-grained materials. Cantré & Saathoff (2011) has numerically formulated a design method for tubes considering the geotextile strain.

Results from a mode geotextile tube test using a large-scale apparatus are presented in this paper. The study was focused on the sedimentation of soil fills and the development of total stresses. The procedures and results are presented in the following sections.

## 2. MATERIALS, LABORATORY SETUP AND METHODS

### 2.1. Fill Material and Geotextile Properties

The model test have been carried out at the geotechnical engineering laboratory at Kunsan National University. The fill material was obtained from a local dredging site in the Saemangeum river estuary near Gunsan City. The physical properties of the dredged fill are shown in Table 1 and its gradation curve is given in Fig 1.

Table 1. Dredged Fill Properties

| Item                                   | Unit | Quantity         |
|--|------|------------------|
| Natural water content, $\omega_n$ (%)  | %    | 15.9             |
| Specific gravity of soil solids, $G_s$ | N/A  | 2.69             |
| Plasticity Index, $PI$ (%)             | %    | NP (Non-Plastic) |
| Percent passing #200 sieve             | %    | 25               |
| Soil classification (USCS)             | N/A  | SM (Silty-Sand)  |

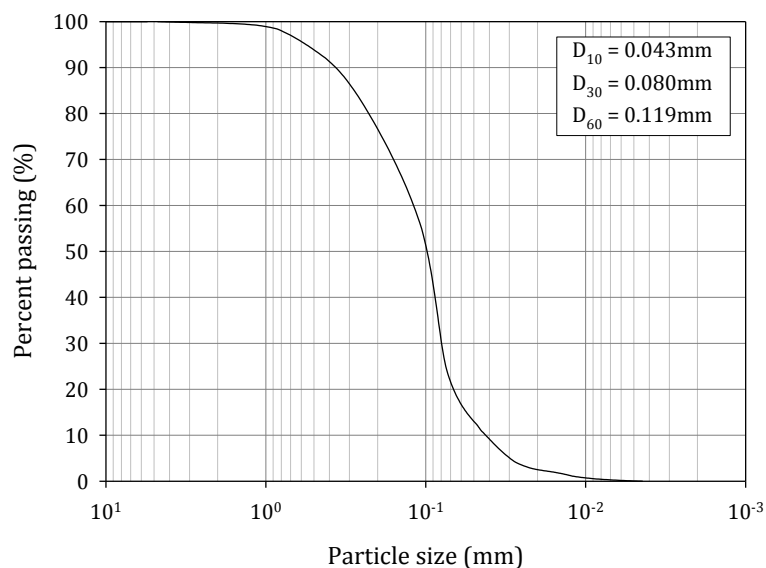


Fig. 1. Gradation Curve

The geotextile tube used in the present study is made of a woven P.P. (polypropylene) geotextile material. The geotextile tube is 4.0 m long and has a theoretical diameter of 1.0 m. The physical properties of the geotextile tube are shown in Table 2. The geotextile tensile strength-strain relationship obtained from a laboratory test of the P.P. material is shown in Fig. 2. Initially the polypropylene geotextile is strained up to 15% with minimal force. This can be attributed to the realignment of loose geotextile fibers at start of the application of the tensile force.

Table 2. Woven Geotextile Properties

| Description/Unit | Unit | Quality/Quantity   |
|------------------|------|--------------------|
| Material Type    | N/A  | PP (Polypropylene) |
| Thickness (mm)   | mm   | 2.0                |
| Tensile Strength | -    |                    |
| Longitudinal     | kN/m | 195                |
| Transverse       | kN/m | 180                |

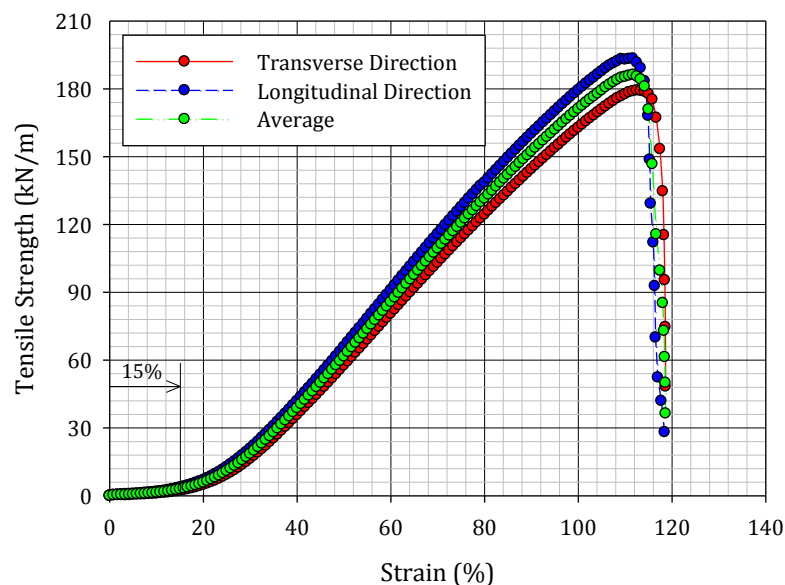


Fig. 2. PP Geotextile Tensile-Strain Curve

## 2.2. Laboratory Setup and Instrumentation

The large-scale apparatus shown in Fig. 3 is equipped with a mixing station, pumping and delivery station, and an observation station. The mixing station comprises of a ① mixing tank and ② water supply tank. Soil (Dredged soil or sand) and water are combined in the mixing tank for the slurry preparation. An electric agitator composed of a shaft rod attached to an electric motor at one end and an impeller at the other end is installed above the mixing tank. The electric agitator blends the soil and water mixture until a slurry material is produced. In the pumping and delivery station a ③ hydraulic pump is used to draw the slurry from the mixing tank via the ④ two-way slurry delivery pipe system during the filling process. There are two filling options for the slurry into the geotextile tube, through direct hydraulic pumping or via the ⑤ gravity tank. For the hydraulic filling, the slurry is hydraulically pumped into the geotextile tube. Alternatively, geotextile filling by gravity initially requires pumping the slurry from the mixing tank to the gravity tank. An electric agitator is also installed on top of the gravity tank to continually agitate the slurry mixture. To fill the geotextile tube, a gate valve at the

bottom of the tank is opened and the slurry is filled through gravitation. In the case of gravity filling, the pumping pressure will be based on the hydraulic head of the slurry in the gravity tank. The hydraulic head will be equal to the difference between the elevation of the filling port and the elevation of the slurry surface. For the present study, the geotextile tubes were filled hydraulically. The experimental observations for the geotextile tube models are made in the observation station or the ⑥ test tank. The steel tank floor have dimensions of 3 m x 5 m and can be filled with water at a maximum height of 1.5 meters to simulate geotextile tube models under submerged conditions. In both submerged and non-submerged geotextile tube test cases, water from the test tank can be recycled and reused for the next experiment by pumping out the water back to the water supply tank using submersible water pumps.

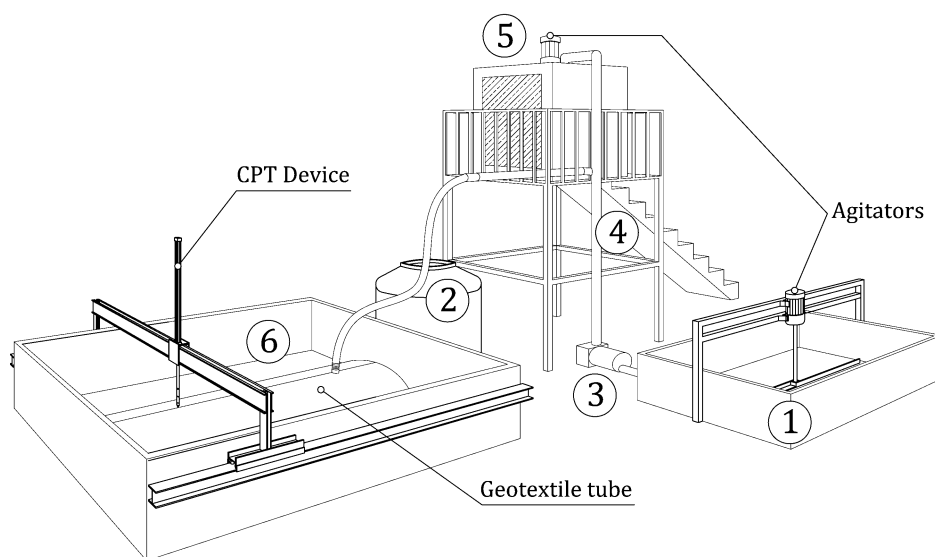


Fig. 3. Laboratory Setup

Strain gauges are also placed on the outer skin of the geotextile. The strain gauge and pressure cell readings were collected by the data logger and interpreted by a desktop computer in the data station. The strain gauge is attached to the geotextile skin in the same manner shown in Fig. 4(a) along the transverse direction of the tube to measure the tube's circumferential strain. The surface of the geotextile area where the strain gauge will be attached should be cleaned. Then a sufficient amount of chloroprene (CR) adhesive (occupies at least about an area of 20 mm x 50 mm) is spread on the surface of the geotextile skin. The strain gauge is then placed on top of the applied CR adhesive. After the strain gauge is secured, an N-1 coating is coated on top of the strain gauge to cover the device. Lastly, the attachment is covered with a VM tape for water proofing. In this study, four strain gauges were attached to the tube in the same manner as shown in Fig. 4(b). Total stress transducers (TST) and strain gauges (SG) were used to monitor the development of stress and strain during the experiment. Details for the location and placement of the pressure and strain sensors are shown in Fig. 5. The schematic of the data station is shown in Fig. 6.

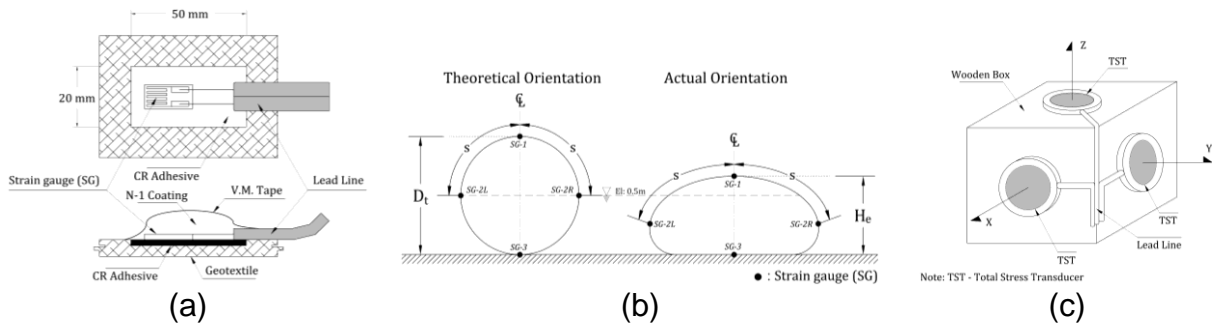


Fig. 4. (a) Strain gauge installation details; (b) strain gauge positioning on the geotextile tube, and; (c) total stress transducer contraction.

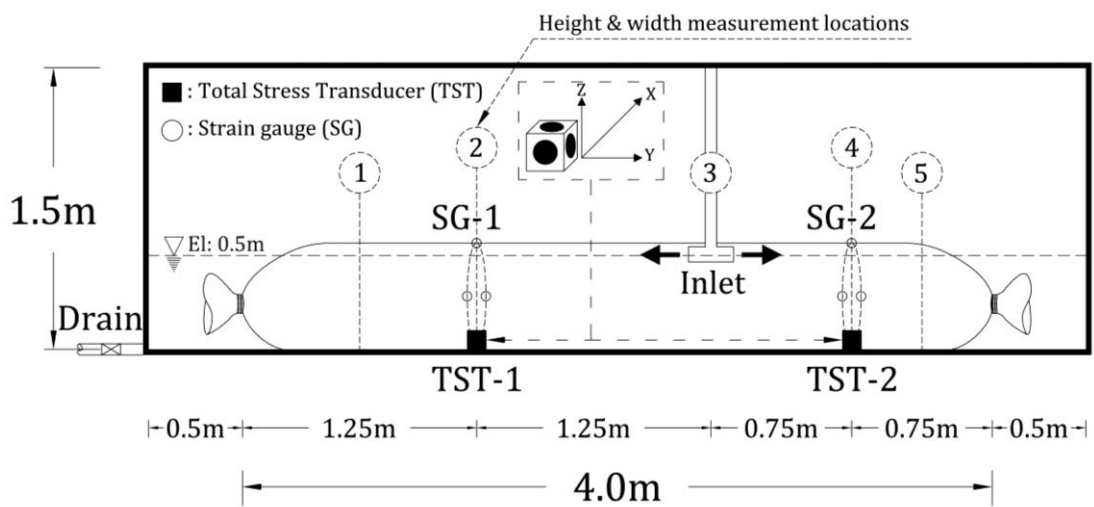


Fig. 5. Instrumentation placement

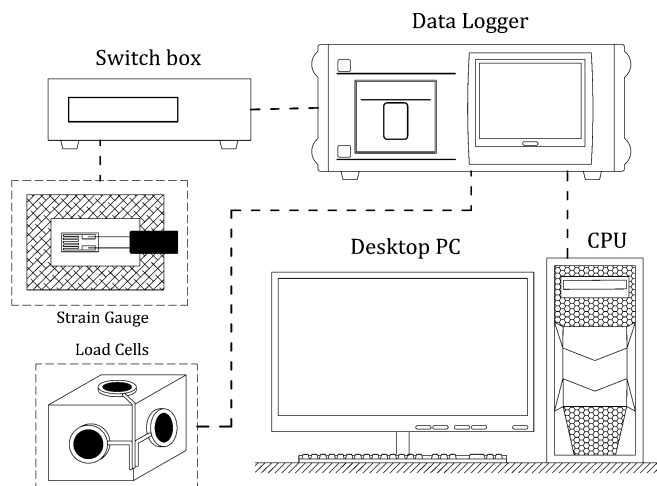


Fig. 6. Instrumentation Setup

### 2.3. Method

For the slurry preparation, the dredged soil and water are combined in the mixing tank. A 3:1 water to soil ratio slurry mixture (300% water content) is used for both geotextile tube experiments. The mixture was continually stirred by the electric agitator to achieve an even mixture and retain the desired slurry consistency. Concurrent with the slurry preparation, the geotextile tube is placed into position inside the test tank. The geotextile tube is filled hydraulically. The slurry is pumped into the geotextile tube through the improvised T-type inlet system during the filling phase. The tubes are filled, dewatered and refilled again until the dewatered height of the tube following the last filling phase is approximately equal to 40 ~ 50% the theoretical diameter of the geotextile tube. The pumping pressure during filling was maintained at 30kN/m<sup>2</sup>. Measurements of the tube height and width at each section are taken after filling (filled height & width) and before refilling (dewatered height & width) of slurry. The strain and pressure data are collected via a data logger and monitored through a desktop PC (Fig. 3). After the filling and dewatering tests, soil samples were gathered from the topmost and bottom part of the tube. The water content and percent passing #200 sieve of these samples were determined to evaluate the variation of fill material characteristics in the tube.

## 3. RESULTS AND DISCUSSIONS

### 3.1. Fill Material and Geotextile Properties

The slurry was hydraulically pumped with slurry ( $\omega = 300\%$ ) at  $Q = 0.0681 \text{ m}^3/\text{min}$  at an average pumping pressure ( $P_0$ ) = 32.96 kPa. The hydraulic pump has a maximum pumping power of 5 HP. In this experiment, four filling stages were conducted. The pumping of slurry were conducted at  $t_1 = 0 \text{ min}$ ,  $t_2 = 40 \text{ min}$ ,  $t_3 = 90 \text{ min}$  and  $t_4 = 150 \text{ min}$ . Each filling stages lasted for approximately 10-15 min. Because the geotextile is permeable, the water is gradually dissipated during the filling process. Hence, no significant loss in the tube height is apparent during the test. Fig. 7 illustrates the variation of the tube sections at Locations ② and ④ (please refer to Fig. 5) and the corresponding tube height and width for each stage are tabulated in Table 3. Evidently the tube height in both sections varies after each filling stage. The variation in the tube height and width can be attributed to the water content and percentages of fine deposits in the area. Laboratory tests on the soil samples, obtained from Locations ② and ④ after the filling and dewatering tests, indicates that Location ② contains less amount of fine particles (17%) and water content (16%) compared to Location ④ where the fine particles are about 25% having a moisture content of about 36%. This also explains why a significant drop in tube height occurred in Location ④, two days after the last filling stage, as shown in Fig. 7(b).

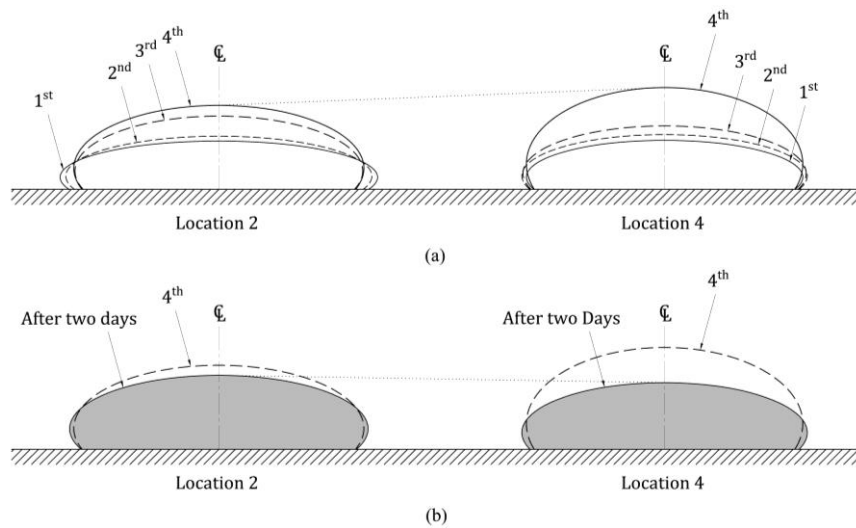


Fig. 7 Geotextile tube shape variation: (a) during filling stages; (b) stabilized stage – two days after the last filling stage

Table 3. Summary of the variation in the geotextile tube's shape properties

| Description | Property    | Filling Stage   |                 |                 |                 | Stabilized Stage<br>(after two days) |
|-------------|-------------|-----------------|-----------------|-----------------|-----------------|--------------------------------------|
|             |             | 1 <sup>st</sup> | 2 <sup>nd</sup> | 3 <sup>rd</sup> | 4 <sup>th</sup> |                                      |
| Location 2  | Height (mm) | 212             | 233             | 321             | 368             | 360                                  |
|             | Width (mm)  | 1390            | 1340            | 1260            | 1265            | 1260                                 |
| Location 4  | Height (mm) | 215             | 240             | 278             | 446             | 292                                  |
|             | Width (mm)  | 1210            | 1250            | 1240            | 1205            | 1245                                 |

### 3.2. Generation of total stress

The total pressure readings are shown in Figs. 15. The recorded readings for Locations ② (TST-1) and ④ (TST-2) are shown Figs. 15(a) and 15(c), respectively (please refer to Fig. 7 for the placement of the sensors). Since the sensitivity of the transducers used in this experiment was about 1 kPa, corresponding data based on polynomial curve fitting is provided in Figs. 15(b) and 15(d) for Locations ② and ④, respectively. Clearly, the pressure readings corresponds to the height of the tube. Interestingly, it appears that the total horizontal pressures (x and y directions, Fig. 6(c) and Fig. 7) are higher than the total vertical pressures. This phenomenon might be due to the confinement effect of the geotextile sheet to the soil sediments inside the geotextile tube. Presumably, due to the increasing geotextile tensile stress, the soil fills are most likely pushed horizontally (inward direction) rather than vertically as shown in Fig. 16.

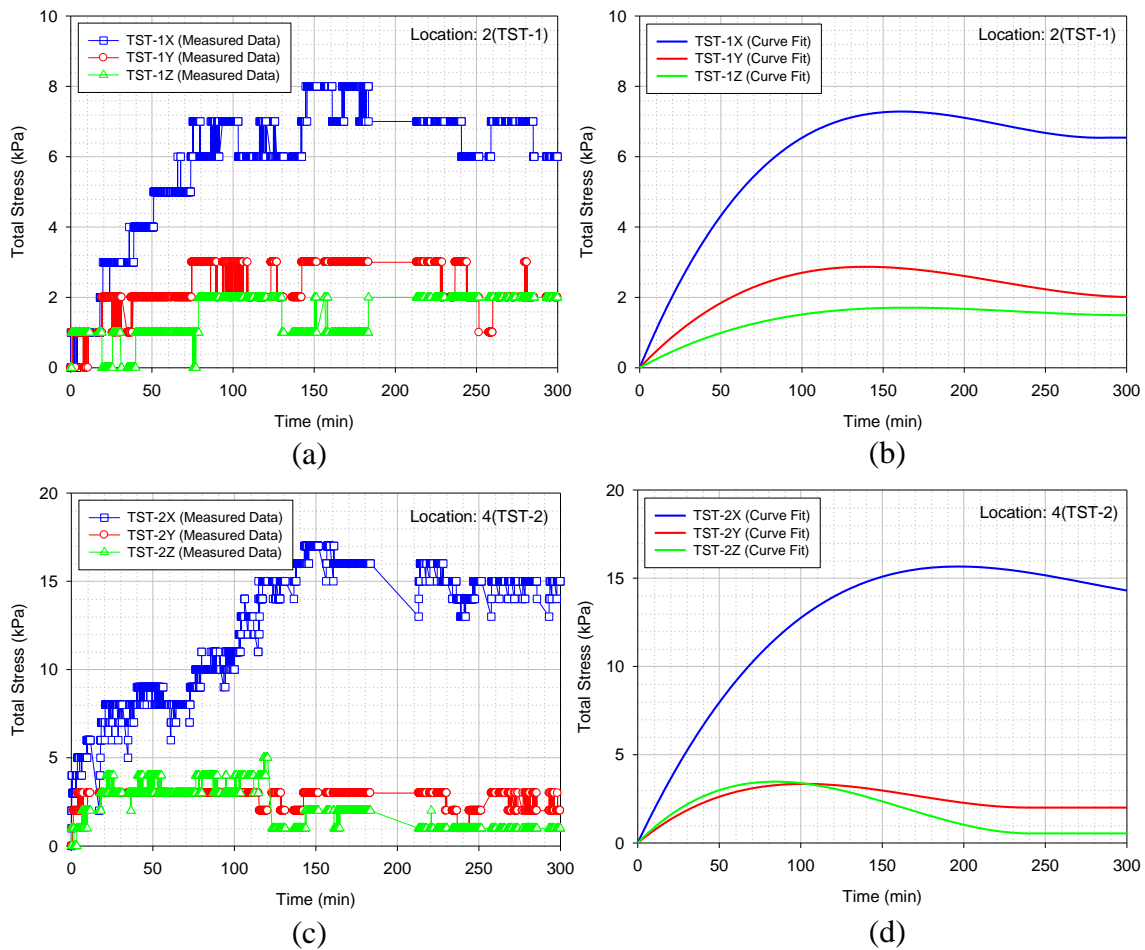


Fig. 15 (a) Total stress readings at Location ②; (b) curve fit for the stress readings at Location ②; (c) total stress readings at Location ④; (d) curve fit for the stress readings at Location ④;

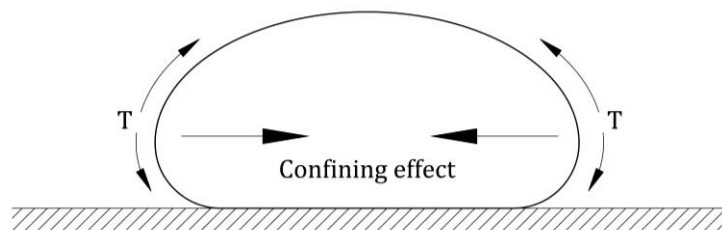


Fig. 16 Geotextile tube's confining effect

In this study, the fill material is assumed to be bounded by a frictionless geotextile membrane. The soil element at any depth in the geotextile tube are subjected to vertical effective pressure,  $\sigma'_v$ , and horizontal effective pressure,  $\sigma'_h$ . The ratio between the effective vertical and horizontal pressures can be defined a non-dimensional  $K$ ,

$$K = \frac{\sigma'_h}{\sigma'_v} \quad (1)$$

The variation in the coefficient of lateral pressures ( $K$ ) at Locations ② and ④ are shown in Fig. 17. Only the coefficients of lateral pressure corresponding to the time at which measurements for the tube height were taken are plotted. In Fig. 17(a), it appears that coefficient of lateral pressure  $K$  of the soil fill at Location ② was increasing during the filling stages and decreased after the last filling stage until it reached steady state. This is reasonable since there was no significant drop in the tube height two days after the last filling stage (refer to Table 3). It might be that the sequence for the lateral earth pressures (total) at Location ② initially began from active state ( $K_a$  condition) during filling, passive state ( $K_p$  condition) during dewatering and then finally reached steady state ( $K_0$  condition). If this is the case for the soil fill at Location ②, then it suggest that the soil fill at Location ④ was still under active state at time  $t = 300$  min. At this point ( $t = 300$  min), the excess pore water pressure at Location ④ is large compared to the soil deposits at Location ②, which at this point has reached steady state. This is why significant loss in the tube height was observed in Location ④ after two days when it finally achieved steady state.

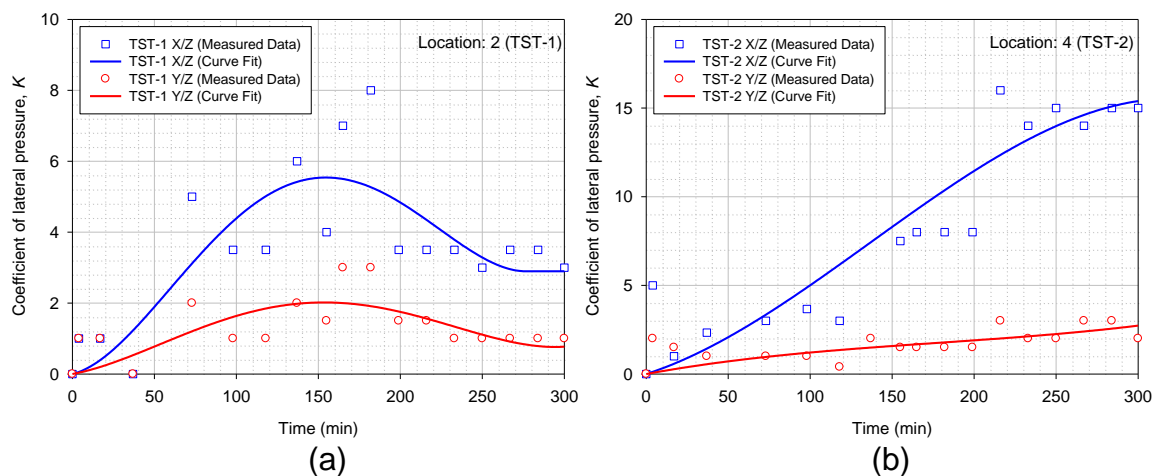


Fig. 17 Coefficient of lateral pressures at (a) Location ② and (b) Location ④

### 3.2. Generation of geotextile strain

During the experiment, the strain gauges were oriented along the transverse direction of the geotextile tube to monitor the development of circumferential strain. The data for the geotextile strain at SG-1 and SG-2 (at Locations ② and ④, respectively, as shown in Fig. 7) are shown in Fig. 18. The readings indicates that the geotextile strain increases during the filling process and decreases during the dewatering process. The sharp spikes can be attributed to the effects of the added pumping pressure during filling. Presumably, minimal geotextile strain occurs at the bottom due to the confining

effect between the soil fill and foundation. During the test, this assumption is proven accurate as represented by the red line in Figs. 18(a) and 18(b) for Locations ② and ④. Due to the confinement of the geotextile in-between the fill material (above) and the foundation (below), the geotextile at the bottom of the tube experience only minimal strain during the filling and dewatering process. Another interesting result of the test is the strain readings at the top and sides of the tube. Both strain gauge readings at Locations ② and ④ suggests that the strain at the sides of the tube are larger compared to the strains at the top. This might seem unlikely, however as previously discussed in section 4.2.2, the magnitude of the total horizontal pressures are larger than the vertical pressures. This implies that the increase in the geotextile strains at the sides of the tube corresponds to the increase in the lateral pressure induced by the fill material.

The existing calculation methods available in the literature assumed that the circumferential tensile force of the geotextile container is constant (Liu & Silvester, 1977; Leshchinsky *et al.*, 1996; Plaut & Suherman 1998). These assumption was made in order to easily solve the plane strain membrane theory problem. For the present study, the reading for the topmost geotextile strain gauge is significantly low for both geotextile containers and the strain gauge data results shows a variation of strain deformation along its circumference. This suggest that in reality the circumferential tensile forces that causes these deformations are non-uniform along the containers circumferential length. It should be noted that the fill material for the geotextile container considered in the theoretical analysis is fluid. Hence, in the case of the present study, the solidified soil fill may have an influence to the strain variation readings on geotextile tube's circumference.

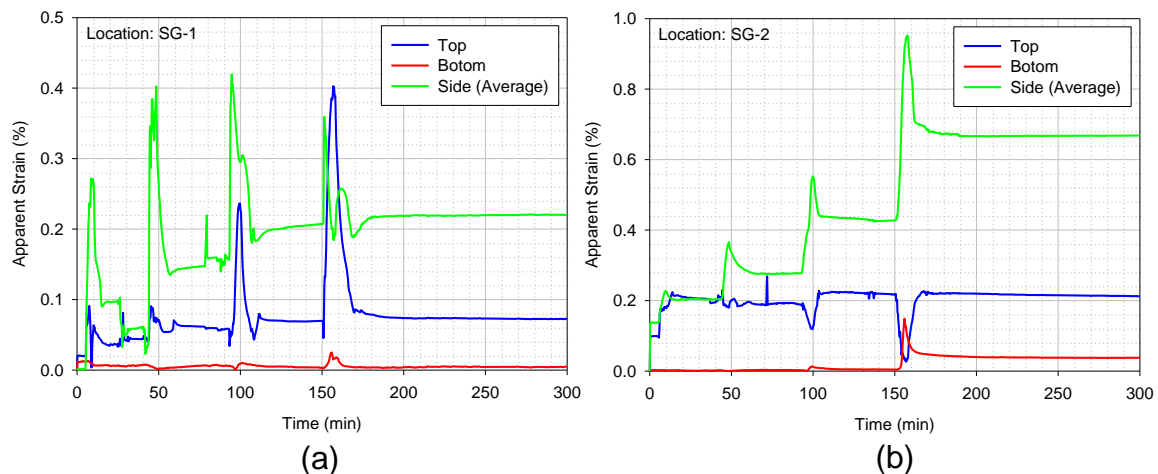


Fig. 18 Strain readings: (a) Location ② (SG-1) and (b) ④ (SG-2)

## 4. CONCLUSIONS

Based on the laboratory tests conducted, the following conclusions are drawn:

- Due to the permeability of the geotextile, the water is gradually dissipated during the filling process. Significant loss in the tube height is not apparent during the test.
- The pressure readings gradually increases with time during the filling process and normalize at the end on the filling stage. Therefore, the recorded pressures directly reflects to the height of the material in the tube.
- Test results indicates that the total horizontal pressures are higher than the total vertical pressures. This phenomenon might be due to the confinement effect of the geotextile sheet to the soil sediments inside the geotextile tube. Presumably, due to the increasing geotextile tensile stress, the soil fills are most likely pushed horizontally (inward direction) rather than vertically.
- Based on the results, it is speculated that the sequence for the lateral earth pressures (total) initially began from active state ( $K_a$  condition) during filling, passive state ( $K_p$  condition) during dewatering and then finally reached steady state ( $K_0$  condition) after the fill materials stabilized.
- The tangential strain of the geotextile tube varies around its circumference.
- The data readings are at minimal at the bottom of the tube. Presumably the stretching of geotextile at these locations are limited due to the confining effect between the soil fill and the foundation.
- The geotextile stains at the sides of the geotextile tube are larger than the geotextile strains at the top. This implies that the increase in the geotextile strains at the sides of the tube corresponds to the increase in the lateral pressure induced by the fill material.
- Due to the variation of the strain distribution on the geotextile skin, the circumferential tensile force of the geotextile may as well be non-constant.

## ACKNOWLEDGEMENTS

This research project is supported by the Technology Advancement Research Program (Grant code: 12TRPI-C064124-01) funded by the Ministry of Land, Infrastructure and Transport in the Republic of Korea.

## REFERENCES

- Alvarez, I. E., Rubio, R. & Ricalde, H. (2007). "Beach Restoration with Geotextile Tubes as Submerged Breakwaters in Yucatan, Mexico." *Geotextiles and Geomembranes*, **25**, 233-241.
- Brink, N.R., Kim, H.J. and Znidarcic, D. (2015). "Numerical Modeling Procedures for Consolidation of Fine-Grained Materials in Geotextile Tubes." *2015 Geosynthetics Conference*, Portland, Oregon, February.

- Brink, N.R., Kim, H.J. and Znidarcic, D. (2013). "Consolidation Modelling for Geotextile Tubes Filled with Fine-Grained Material." *GhIGS GeoAfrica 2013 Conference*, Accra, Ghana, November.
- Cantré, S. 2002. "Geotextile Tubes – Analytical Design Aspects." *Geotextiles and Geomembranes*, **20**, p. 305-319.
- Cantré, S. & Saathoff, F. (2011). "Design Method for Geotextile Tubes Considering Strain – Formulation and Verification by Laboratory Tests using Photogrammetry." *Geotextiles and Geomembranes*, **29**, 201-210.
- Fowler, J., Ortiz, C., Ruiz, N. & Martinez, E. (2002a). "Use of geotubes in Columbia, South America." *Proceedings of the 7th International Conference on Geosynthetics*, Nice, France, Balkema, **3**, p. 1129–1132.
- Fowler, J., Stephens, T., Santiago, M. & De Bruin, P. (2002b). "Amwaj Islands constructed with Geotubes, Bahrain." *CEDA Conference*, Denver, USA, pp. 1–14.
- Gibeaut, J. C., Hepner, T. L., Waldinger, R., Andrews, J. R., Smyth, R. C., Gutierrez, R., Jackson J. A. & Jackson, K. G. (2003). "Geotubes for Temporary Erosion Control and Storm Surge Protection along the Gulf of Mexico Shoreline of Texas." *Proc. 13th Biennial Coastal Zone Conference*, Baltimore, MD, CD-ROM.
- Kim, H.J., Lee, K.W., Jo, S.K., Park, T.W. & Jamin, J.C. (2014a). "The Influence of Filling Port System to the Accretion and Pressure Distribution of Dredged Soil Fill in Acrylic Tubes." *Proc. Advances in Civil, Environmental and Materials Research (ACEM14)*, Busan, Korea, CD-ROM.
- Kim, H., Won, M., and Jamin, J. (2014b). "Finite-Element Analysis on the Stability of Geotextile Tube–Reinforced Embankments under Scouring." *Int. J. Geomech.* , 10.1061/(ASCE)GM.1943-5622.0000420 , 06014019.
- Kim, H.J., Won, M.S., Kim, Y.B., Choi, M.J. & Jamin, J.C. (2014c). "Experimental Analysis on Composite Geotextile Tubes Hydraulically Filled Underwater Condition." *Proc. Advances in Civil, Environmental and Materials Research (ACEM14)*, Busan, Korea, CD-ROM.
- Kim, H. J., Jamin, J. C. & Mission, J. L. (2013a). "Finite Element Analysis of Ground Modification Techniques for Improved Stability of Geotubes Reinforced Reclamation Embankments Subjected to Scouring." *Proc. Advances in Structural Engineering and Mechanics (ASEM13)*, Jeju, Korea, p. 2970-2979.
- Kim, H.J., Jamin, J.C., Won, M.S., Sung, H.J. & Lee, J.B (2013b). "A Study on the Behavior of Dredged Soil Stratified in a Transparent Geobag." *Proc. Advances in Structural Engineering and Mechanics (ASEM13)*, Jeju, Korea, p. 2980-2987.
- Koerner, G. R. & Koerner, R. M. (2006). "Geotextile Tube Assessment Using a Hanging Bag Test." *Geotextiles and Geomembranes*, **24**, 129-137.
- Kriel, H. J. (2012). "Hydraulic Stability of Multi-Layered Sand-Filled Geotextile Tube Breakwaters under Wave Attack." MSc Thesis, Stellenbosch University, South Africa.
- Lawson, C. R. (2008). "Geotextile Containment for Hydraulic and Environmental Engineering." *Geosynthetics International*, **15**(6), 384-427.
- Leshchinsky, D., Leshchinsky, O., Ling, H. I. & Gilbert, P. A. (1996). "Geosynthetic Tubes for Confining Pressurized Slurry: Some Design Aspects." *Journal of Geotechnical Engineering*, pp. 682-690.
- Liu, G. S. & Silvester, R. (1977). "Sand Sausages for Beach Defence Work." *6th*

*Australasian Hydraulics and Fluid Mechanics Conference*, pp. 340-343.

- Moo-Young, H. K., Gaffney, D. A. & Mo, X. (2002). "Testing Procedures to Assess the Viability of Dewatering with Geotextile Tubes." *Geotextiles and Geomembranes*, **20**, 289-303.
- Parab, S. R., Chodankar, D. S., Shirgaunkar, R. M., Fernandes, M., Parab, A. B., Aldonkar, S. S. & Savoikar, P. P. (2011). "Geotubes for Beach Erosion Control in Goa." *International Journal of Earth Sciences and Engineering*, **4**, p. 1013-1016.
- Pilarczyk, K. W. (2008). "Alternatives for Coastal Protection." *Journal of Water Resources and Environmental Engineering*, **23**, p. 181-188.
- Plaut, R. H. & Klusman, C. R. (1999). "Two-dimensional Analysis of Stacked Geosynthetic Tubes on Deformable Foundations." *Thin-walled Structures*, **34**, p. 179-194.
- Plaut, R.H. and Suherman, S. (1998). "Two-dimensional Analysis of Geosynthetic Tubes." *Acta Mechanica*, 129(3-4), 207-218.
- Recio, J. & Oumeraci, H. (2009). "Processes Affecting the Hydraulic Stability of Coastal Revetments made of Geotextile Sand Containers." *Coastal Engineering*, **56**, p. 260-284.
- Restall, S. J., Jackson, L. A., Heerten, G. & Hornsey, W. P. (2002). "Case Studies Showing the Growth and Development of Geotextile Sand Containers: An Australian Perspective." *Geotextile and Geomembranes*, **20**, p. 321-342.
- Weggel, J. R., Dortch, J. & Gaffney, D. (2011). "Analysis of Fluid Discharge from a Hanging Bag." *Geotextiles and Geomembranes*, **29**, 65-73.
- Vashi, J.M., Desai, A.K. and Solanki, C.H. (2013). "Behavior of geotextile reinforced flyash + clay-mix by laboratory evaluation." *Geomechanics and Engineering*, **5**(4), 331-342.